Basic Study on Energy-optimized Speed Trajectory for Electric Vehicles between Traffic Signals Based on Stochastic Model Using Low Frequency Floating Car Data

Yuki Hosomi*a) Non-member, Shota Yamada* Member
Binh Minh Nguyen* Member, Sakahisa Nagai* Member
Hiroshi Fujimoto* Senior Member

Energy-efficient driving is required in aiming for a low-carbon society. This study aims to obtain the optimal speed trajectory by a stochastic model derived from floating car data. In this paper, the time required to reach the next traffic light and the probability of passing through it are estimated by a Gaussian mixture model (GMM) based on the data, and dynamic programming (DP) is utilized to minimize the energy cost function. This proposed approach enables the calculation of optimal speed trajectories where there is no vehicle communication and traffic signals cannot be detected by an onboard vision system. Simulation results demonstrate that the proposed system reduces the energy required to reach the next traffic light by 2.4 % in comparison with human driving.

Keywords: electric vehicle, energy-optimized speed trajectory, stochastic model, signalized intersections, dynamic programming

1. Introduction

1.1 Energy Efficient Driving Electric vehicles (EVs) are gaining more attention and the number of EVs around the world is increasing. The fast response of motors and low greenhouse gas emissions in life cycle assessments [(1)] are the advantages of EVs. On the other hand, range limitations due to the low energy density of the battery and long charging time are the problems of EVs. Since range extension simultaneously reduces driving costs and greenhouse gas emissions, many studies have been done in various environments and situations, like on highways [(2)], following a preceding car [(3)], and passing traffic signals [(4)~(6)].

Due to the range limitations, EVs are well suited for use in inner-city environments. Therefore, this study focuses on the inner-city road, but many stops and accelerations are required due to traffic signals, congestion, pedestrians, etc. Especially, traffic signals are a major cause of stops. Thus, it is important to consider the traffic signal constraints in generating the optimal speed trajectory on urban roads.

1.2 Optimal Trajectory Considering Traffic Signals To minimize energy for passing traffic signals, two different methods, integrated traffic signal control and optimal speed trajectory of individual vehicles, are used. The subject of this study is to obtain an energy-optimized speed trajectory.

In many previous studies, traffic signal information is given by Vehicle-to-Infrastructure communication (V2I). Assuming V2I is available, there are previous studies that consider multiple signals [(4)(5)], models that consider vehicle waiting queues before signals [(7)], and models that consider V2I uncertainty in a probabilistic model. Some studies consider surrounding vehicles by using vehicle-to-vehicle communication (V2V) [(8)].

However, V2I and V2V have not yet been put into practical use, and there are also issues such as communication delays and communication failures. Then, some studies have proposed methods not to rely on V2I or V2V. For instance, based on seld-driving data and the detection position of traffic signal state changes, a stochastic model has been used to predict the time to pass through the next traffic signal [(9)].

1.3 Traffic Flow Estimation Using Data As the information society progresses, vehicle transit data is being accumulated and used to estimate urban traffic flow. To collect a wide range of transit data, this research uses low-frequency floating car data like ETC2.0 probe information [(10)]. The data is used to estimate the urban link travel time [(11)] and to estimate traffic signal information, such as the cycle and split time of a single traffic signal [(12)(13)].

The above studies aim at estimating the travel time and the signal information, and none of them model the traffic flow between traffic signals to derive the optimum speed trajectory for each vehicle. This study attempts to model the traffic flow suitable for deriving the optimum speed trajectory between traffic signals.

1.4 Paper Contributions This paper proposes a new method to optimize the vehicle speed trajectory from floating car data without utilizing V2V and V2I. For simplicity, this study targets the modeling of the relationship between adjacent traffic signals. A GMM estimates the probability distribution of the average speed between signals based on floating car data, and DP generates the optimal speed trajectory by using the estimated speed and the passing probability from the probability distribution. Using the proposed method, the

a) Correspondence to: hosomi.yuki22@ae.k.u-tokyo.ac.jp
* The University of Tokyo
5-1-5, Kashiwanoha, Kashiwa, Chiba, 277-8561 Japan

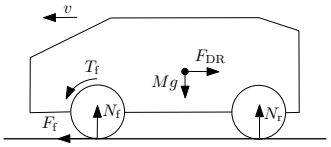

Fig. 1. Modeling of an EV with front IWMs.

expected energy consumption between adjacent signals is reduced.

2. Modeling

2.1 Vehicle Model Fig. 1 shows the force analysis of an EV with front in-wheel motors (IWMs). In this research, only the straight driving condition is considered. The equations that describe the rotational motion of the wheel and the motion of the vehicle are expressed as

$$J_{\omega f}\frac{d\omega_i}{dt} = T_i - rF_i,\ i = \{\mathrm{fl}, \mathrm{fr}\}, \quad \cdots\cdots (1)$$

$$M\frac{dv}{dt} = F_{\mathrm{fl}} + F_{\mathrm{fr}} - F_{\mathrm{DR}}, \quad \cdots\cdots (2)$$

where $J_{\omega f}$, F_i, F_{DR}, v, ω, r, and M are the front wheel's moment of inertia, the driving force, the dragging force, vehicle speed, wheel speed, wheel radius, and vehicle mass, respectively.

The driving force F_f and the load force of the front N_f are given as (3) and (4). Since only a high-μ road surface is considered, the driving force can be approximately expressed by the driving stiffness coefficient D_s and the slip ratio λ.

$$F_f \simeq D_s N_f \lambda, \quad \cdots\cdots (3)$$

$$N_f = \frac{1}{2}\left(\frac{l_r}{l}Mg - \frac{h_g}{l}M\frac{dv}{dt}\right), \quad \cdots\cdots (4)$$

$$\lambda_i = \frac{\omega_i r - v}{\max(\omega_i r, v, \epsilon)}, \quad \cdots\cdots (5)$$

where l, l_r, h_g, and ϵ are wheelbase, distance from the center of gravity (CG), the height of CG, and a small positive number to prevent division by zero, respectively.

The dragging force is given as (6), which is the sum of air resistance and rolling resistance.

$$F_{\mathrm{DR}} = \mu_r Mg + b|v| + F_a v^2, \quad \cdots\cdots (6)$$

where μ_r, b, and F_a are the rolling resistance coefficient, viscous resistance coefficient, and air resistance coefficient, respectively.

Based on the above equations, the IWM torque is expressed as follows:

$$T_i = \frac{rF_{\mathrm{DR}} + M\frac{dv}{dt}}{2} + J_{\omega f}\frac{d\omega_i}{dt}. \quad \cdots\cdots (7)$$

Besides, the relationship between the wheel speed and the vehicle speed can be derived as

$$\omega_i = (1+\lambda_i)\frac{v}{r}. \quad \cdots\cdots (8)$$

2.2 Modeling of Inverter Input Power The inverter input power is given as (9). In this study, the inverter loss and the mechanical loss of the motor are neglected.

$$P_{\mathrm{in}} = P_{\mathrm{out}} + P_{\mathrm{cu}} + P_{\mathrm{fe}}. \quad \cdots\cdots (9)$$

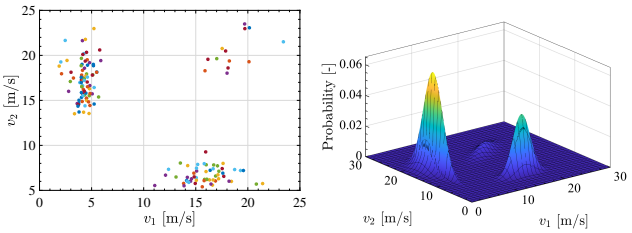

(a) Scatter plots of v_1 and v_2. (b) The fitted result of Fig. 2(a).

Fig. 2. Actual floating car data and the fitted result.

The input power is the sum of output power P_{out}, copper loss P_{cu}, and iron loss P_{fe}, where $|I_d| << |I_q|$ is assumed [14]. Assuming that the motors are of permanent magnet synchronous types, each of them is defined as

$$P_{\mathrm{out}} = \sum_{\mathrm{all}} \omega_i T_i, \quad \cdots\cdots (10)$$

$$P_{\mathrm{cu}} = \sum_{\mathrm{all}} \frac{3}{2}R\left(\frac{T_i}{K_t}\right)^2, \quad \cdots\cdots (11)$$

$$P_{\mathrm{fe}} = \sum_{\mathrm{all}} \frac{3}{2}\frac{(\omega_i p_n)^2}{R_{ci}}\left(L_q^2\left(\frac{T_i}{K_t} - \frac{\omega_i p_n \Psi}{R_{ci}}\right)^2 + \Psi^2\right), \quad (12)$$

where K_t, p_n, R, L_q, and Ψ are motor constant, number of pole pairs, copper resistance, q-axis inductance, and leakage flux, respectively. Equivalent iron loss resistance R_c is given as

$$\frac{1}{R_{ci}} = \frac{1}{R_{c0}} + \frac{1}{R_{c1}|\omega_i p_n|}, \quad \cdots\cdots (13)$$

where R_{c0} and R_{c1} are both equivalent iron loss resistances.

2.3 Proposed Stochastic Traffic Flow Model The relationships between adjacent signals are estimated by floating car data. To model the relationship between each adjacent traffic signal pair, the average speed in front of the first traffic signal v_1 and the average speed between signals v_2 are measured and plotted as a scatter plot. Distribution plots of average speeds using actual floating car data are shown in Fig. 2(a). Position data every 200 m of vehicles equipped with ETC2.0 measured in Chiba, Japan in September 2019 is used as floating car data. In this case, the distance between signals is about 650 m.

Due to the stopping and passing of traffic signals, the scatter has some clusters as shown in Fig. 2(a). Thus, the GMM is used to describe the data and is given as

$$p(X) = \Sigma_{k=1}^{n} \pi_k N(X \mid \mu_k, \Sigma_k), \quad \cdots\cdots (14)$$

$$N(X \mid \mu_k, \Sigma_k) = (2\pi \mid \Sigma_k \mid)^{-\frac{1}{2}} e^{\{(-\frac{1}{2})(X-\mu_k)^T \Sigma_k^{-1}(X-\mu_k)\}}, \quad (15)$$

$$X = [v_1\ v_2]^{\mathsf{T}}, \quad \cdots\cdots (16)$$

where μ_k, Σ_k, and π_k are the mean, variance, and mixing coefficient, respectively. The fitted results of Fig. 2(a) are shown in Fig. 2(b). Using these data, the probability distribution of v_2 is numerically calculated.

3. Proposed Trajectory Generation

3.1 Optimization Problem The optimization problem to minimize energy is as follows. The objective function is the power consumption required for driving and the constant accessory power loss. The final step L is calculated by

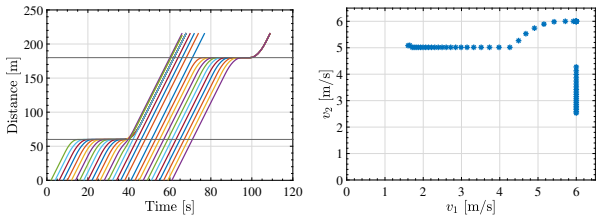

(a) Vehicle trajectory. (b) Average speed scatter plot.

Fig. 3. Traffic flow: distance is 120 m

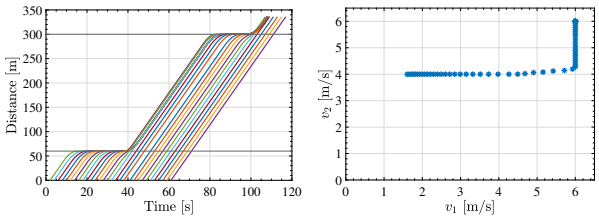

(a) Vehicle trajectory. (b) Average speed scatter plot.

Fig. 4. Traffic flow: distance is 240 m

the estimated $\hat{v}_2$ from the GMM presented in the previous section.

$$\min_{v(k)} \mathrm{E}\left[\sum_{k=0}^{L}(P_{\mathrm{in}}(k)\Delta t + \alpha\Delta t) - \phi(v(L))\right], \quad \cdots\cdots\cdots (17)$$

$$\text{s.t.:} \quad v_{\min} \le v(k) \le v_{\max}, \quad \cdots\cdots\cdots (18)$$

$$T_{\min} \le T(k) \le T_{\max}, \quad \cdots\cdots\cdots (19)$$

$$x(k+1) = x(k) + \frac{v(k+1)+v(k)}{2}\Delta t, \quad \cdots\cdots (20)$$

$$P_{\mathrm{in}}(k) = P_{\mathrm{out}}(k) + P_{\mathrm{cu}}(k) + P_{\mathrm{fe}}(k), \quad \cdots\cdots\cdots (21)$$

$$\Delta t = 1,\ L = \frac{d}{\hat{v}_2}, \quad \cdots\cdots\cdots (22)$$

$$v(0) = v_{\mathrm{start}},\ v(L) = \hat{v}_{\mathrm{end}}, \quad \cdots\cdots\cdots (23)$$

$$x(0) = 0,\ x(L) = d, \quad \cdots\cdots\cdots (24)$$

where E denotes the expected value, and d, α, and $\phi(v(L))$ are the distance between signals, constant accessory power, and cost function based on termination kinetic energy, respectively. As the boundary condition of speed, v_{start} is the input variable, and $\hat{v}_{\mathrm{end}}$ is the estimated terminal speed.

In this study, the accessory power consumption is set to 500 W. Taking into account power consumption proportional to time, there exists a speed at which the power consumption is minimized in steady-state driving.

3.2 Classification of Average Speed Distribution When passing through the first signal, speed distributions can be classified into two categories based on the relationship between the two traffic signals. The vehicle trajectories and average speed distributions for 120 m and 240 m between signals at a signal cycle of 60 s, a split time of 30 s, and a constant speed of 6 m/s are shown in Figs. 3(a), 3(b), 4(a), and 4(b), respectively. When distance between traffic signals is 120 m, the distribution of v_2 separates, where v_1 is 6 m/s. On the other hand, it does not separate when the distance between signals is 240 m. Without signal information, some cars may stop in front of a traffic signal for a long time and travel unnecessarily fast. The proposed method estimates v_2 to reduce power consumption by eliminating unnecessary acceleration/deceleration.

3.3 Proposed Algorithm Fig. 5 shows the flowchart for deriving the optimum speed trajectory. First, floating car data is obtained and v_1 and v_2 are measured and plotted on a two-dimensional scatter plot. Next, using the method described in subsection 2.3, the speed distribution map is modeled using the GMM, and the probability density distribution of v_2 is obtained when v_1 is given as the input variable. There are two different methods to be applied depending on whether the probability distribution is separated. Whether the speed distributions are separated depends on whether the passing

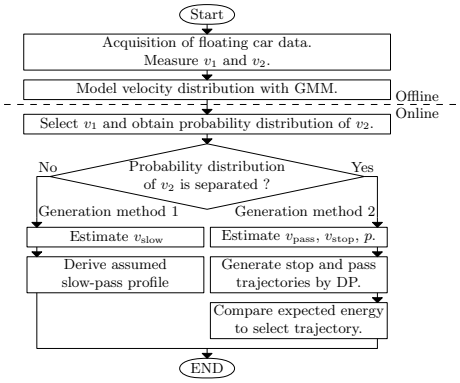

Fig. 5. Flowchart of the proposed algorithm.

signal cycles are identical or separated. Both of the two methods use DP to solve the optimization problem which is presented in subsection 3.1 and generate an optimized trajectory by using the estimated average speed from GMM.

When the probability distribution is not separated, the speed trajectory is obtained by generation method 1, and when the speed distribution is separated, it is generated by generation method 2.

3.3.1 Generation Method 1 To solve the optimization problem by DP, the average speed between signals $\hat{v}_{\mathrm{slow}}$ is determined. The $\hat{v}_{\mathrm{slow}}$ is determined as the speed at which the cumulative distribution function of v_2 is k. k is a design parameter, and if k is large, $\hat{v}_{\mathrm{slow}}$ is large. In this paper, k is 0.25, which is to prevent deceleration due to early arrival at the second signal. Selecting $\hat{v}_{\mathrm{slow}}$ as $\hat{v}_2$ and $\hat{v}_{\mathrm{end}}$, the possible optimized speed trajectory is shown in Fig. 6(a).

3.3.2 Generation Method 2 When the probability distribution of v_2 is separated, two different average speeds between signals are estimated, $\hat{v}_{\mathrm{pass}}$ is assumed to pass and $\hat{v}_{\mathrm{stop}}$ is assumed to stop. The trajectory is selected by evaluating the expected energy using the passing probability p derived from the GMM.

$\hat{v}_{\mathrm{stop}}$ and $\hat{v}_{\mathrm{pass}}$ can be defined as the v_2 at which each of the separate cumulative distribution function of v_2 is 0.5, where $\hat{v}_{\mathrm{stop}} < \hat{v}_{\mathrm{pass}}$. p is calculated as the ratio between the area of the probability distribution assumed to pass and the overall area.

Using $\hat{v}_{\mathrm{stop}}$ and $\hat{v}_{\mathrm{pass}}$, DP generates the two optimal trajectories. The terminal velocity is set to v_{pass} for the pass trajectory and 0 for the stop trajectory. Fig. 6(b) shows the possible three trajectories when the probability distribution is separated. It consists of speed trajectories generated by the DP using $\hat{v}_{\mathrm{stop}}$ and $\hat{v}_{\mathrm{pass}}$ and a speed trajectory that is assumed to pass but fails to pass. The power consumption calculated from DP is represented by $\hat{J}_{\mathrm{pass}}$, $\hat{J}_{\mathrm{fail}}$, and $\hat{J}_{\mathrm{stop}}$, re-

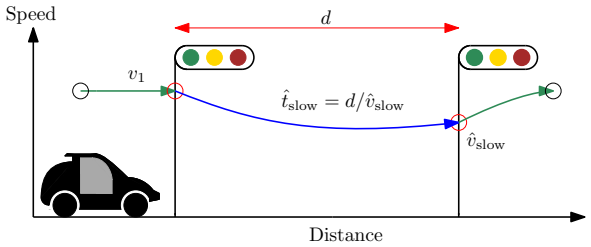

(a) Generation method 1.

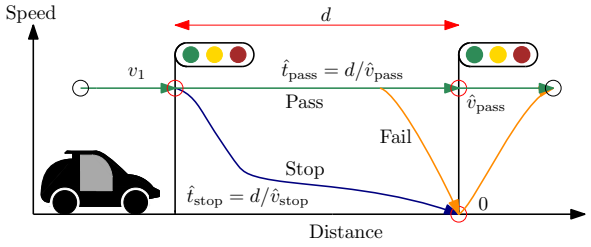

(b) Generation method 2.

Fig. 6. Possible optimized speed trajectory.

Fig. 7. Experimental vehicle (FPEV2-Kanon).

Table 1. Vehicle Specification.

Parameter	Value
M	860 kg
h_{g}	0.51 m
$l,\ l_{\mathrm{r}}$	1.715 m, 0.702 m
μ_{r}	0.01
b	15.4 kg/s
F_{a}	0.105 $\mathrm{Ns^2/m^2}$
$J_{\omega\mathrm{f}}$	1.24 $\mathrm{kgm^2}$
D_{s}	10

Table 2. Specification of IWM.

Parameter	Value
L_q	690 µH
Ψ	0.18 Wb
R	0.06 Ω
R_{c0}	300 Ω
R_{c1}	0.13 Ω
p_{n}	10
K_{t}	1.8 Nm/A
r	0.301 m

spectively. The speed trajectory of the human-operated vehicle that forms the floating car data is considered to be a passing trajectory. The proposed method adds a speed trajectory that decelerates in advance assuming a stop, and the choice between the pass or stop trajectory is decided by comparing the expected value of power consumption. Using the passing probability estimated from the GMM, the expected energy value of the assumed passing trajectory can be expressed by the following equation:

$$\mathrm{E}[\hat{J}_{\mathrm{exp}}] = p\hat{J}_{\mathrm{pass}} + (1-p)\hat{J}_{\mathrm{fail}}. \quad \cdots\cdots\cdots\cdots\cdots\cdots (25)$$

Then, $\mathrm{E}[\hat{J}_{\mathrm{exp}}]$ and $\hat{J}_{\mathrm{stop}}$ are compared, and the trajectory with the smaller energy consumption is selected.

4. Evaluation Test

4.1 Evaluation Setting To evaluate the proposed method, a simulator is made based on the electric vehicle FPEV2-Kanon (Fig. 7). The main parameters of the vehicle and the IWM are summarized in Tables 1 and 2, respectively. The simulation setting is as follows. The traffic light cycle is 60 s, and the green and red durations are 30 s. The onboard camera can detect the traffic signal within 24 m of the traffic signal, and the vehicle controller decides to pass or stop. Assuming uncrowded road conditions, the vehicle can freely determine its speed between a minimum and a maximum speed. The data used for learning the GMM is generated as a constant acceleration/deceleration trajectory with no prior signal information that simulates human driving, and the constant acceleration/deceleration is decided by the onboard camera information. It is assumed that the starting time to approach the first signal is random. As indicated in the speed trajectory generation method, the speed trajectory generation method differs depending on the distance between signals and is therefore verified separately. Four cases which are shown in Table 3 are verified.

Table 3. Simulation Verification Cases.

Case	Description
1	Comparison: proposed method and no-control when stops at the first signal Distance: 60 m, Offset time: 30 s, Method 1
2	Comparison: proposed method and no-control when passing the first signal Distance: 240 m, Offset time: 0 s, Method 1
3	Comparison: pass and stop trajectories when passing the first signal Distance: 120 m, Offset time: 0 s, Method 2
4	Comparison: power consumption of stop and pass trajectories Distance: 120, 420, 480 m, Offset time: 0 s, Method 2

4.2 Results and Discussion

Case 1 The figures of the speed trajectory, transit trajectory, and energy are shown in Figs. 8(a), 8(b), and 8(c), respectively. The proposed method reduces power consumption by 28 % and 26 % compared to without-control and DP without GMM, respectively.

Case 2 The vehicle trajectories without control and with the proposed method 1 (DP+GMM) are shown in Figs. 9(a) and 9(b), respectively. A comparison of the power consumption of no-control and the proposed trajectory for starting time is shown in Fig. 9(c). The expected power consumption is 116.6 kJ for the no-control trajectory and 113.8 kJ for the proposed method, thus the power consumption is reduced by 2.4 %.

Case 3 Figs. 10(a) and 10(b) show the assumed pass and stop trajectories, respectively. Without control, only the pass trajectory is considered, but the proposed method allows the stop trajectory to be considered. Fig. 10(c) shows the power consumption at each starting time. When the starting time is small, the pass trajectory consumes less energy. On the other hand, when the starting time is large, sudden deceleration can be prevented and power consumption can be reduced by the proposed stop trajectory.

Case 4 Figs. 11(a), 11(b), and 11(c) show the comparison of the passing probability of the second signal and power consumption when the distance between signals is 120, 420, and 480 m, respectively. This case compares the energy estimated by the proposed method 2 ($\mathrm{E}[\hat{J}_{\mathrm{exp}}]$ and $\hat{J}_{\mathrm{stop}}$) and that obtained from the simulation for both the assumed stop and pass trajectories. As the distance between signals increases, the range of the passing probability where the power consumption of the stop trajectory is smaller than that of the pass trajectory becomes larger. Since the passing probability is obtained from the GMM, the estimated value by the proposed method matches the simulation value when a pass is assumed, but when a stop is assumed, the passing probability cannot be obtained and the estimated result does not

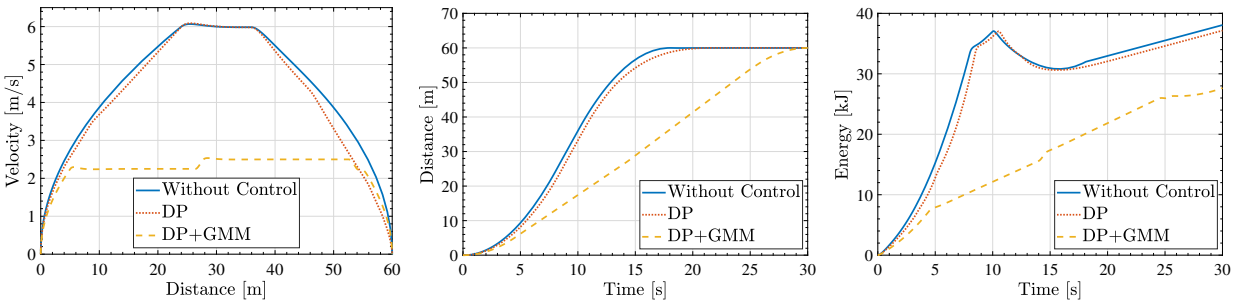

(a) Speed Trajectory. (b) Vehicle Trajectory. (c) Energy consumption.

Fig. 8. Simulation result (Case 1).

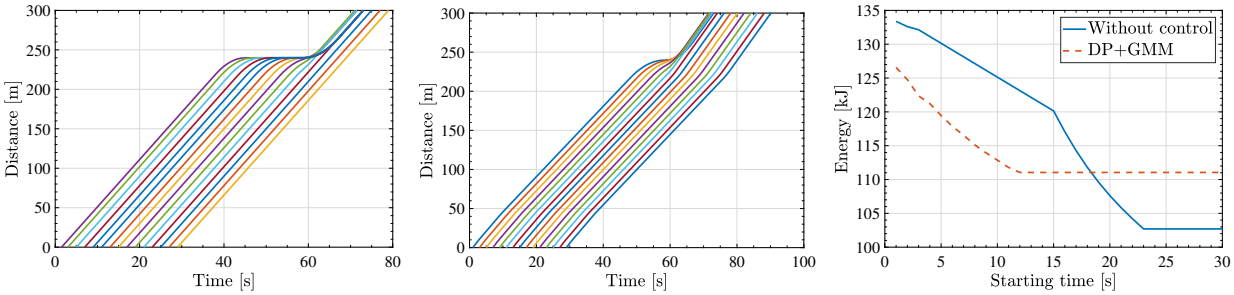

(a) Vehicle trajectory without Control. (b) Vehicle trajectory with DP+GMM. (c) Energy consumption.

Fig. 9. Simulation result (Case 2).

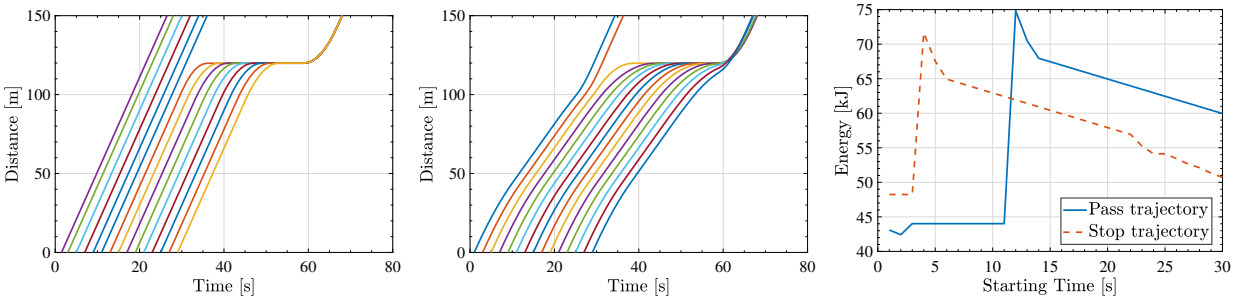

(a) Pass trajectory. (b) Stop trajectory. (c) Energy Comparison.

Fig. 10. Simulation result (Case 3).

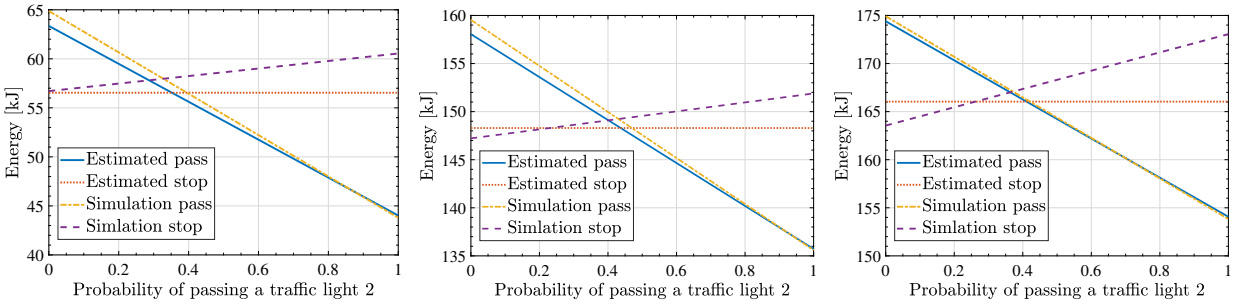

(a) Distance between signals: 120 m. (b) Distance between signals: 420 m. (c) Distance between signals: 480 m.

Fig. 11. Simulation result (Case 4).

match that of simulation at large passing probability.

Discussion When the vehicle stops at both adjacent traffic signals, it is possible to design the speed trajectory so that the vehicle reaches the next traffic signal when the signal turns green, thereby greatly reducing power consumption.

The proposed method can reduce energy consumption when the speed distributions are not separated. Although there are cases in which the proposed method cannot reduce power consumption depending on the starting time, the expected value of power consumption is reduced by the proposed method, confirming the effectiveness of the proposed method.

When the speed distributions are separated, the lower power consumption speed trajectory depends on the start

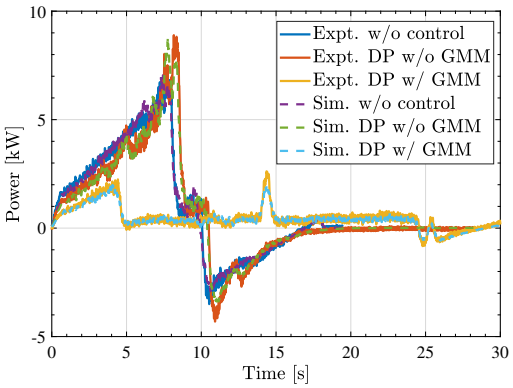

Fig. 12. Experimental comparison of power consumption. Expt. and Sim. denote the experimental and simulation value, respectively.

time. Therefore, the applicability of the stop trajectory depends on the passing probability. It is important to estimate the expected power consumption by the proposed method to properly select the pass or stop trajectory. Although there are errors in the power consumption obtained by the simulation and the proposed method, the error is small in the intermediate region of the passing probability where the energy of the pass and stop trajectories is equal. Thus, the simulation confirmed that the proposed method can select the stop and pass trajectory. The aforementioned results verify the effectiveness of the proposed method in reducing energy consumption by (i) taking into account the assumed stop trajectory; (ii) selecting between the pass and stop trajectory.

4.3 Experimental Validation The speed trajectory of Case 1 is given to the actual vehicle and the inverter input power is measured. For each speed trajectory, the experiment is performed five times. The measured power is compared with the estimated power based on the inverter input power model using measured wheel speed and both are shown in Fig. 12.

The experimental values are in agreement with the power model used in the simulation. Compared to total power consumption, the difference between the actual and the calculated power is less than 6.6 %. The agreement between the power consumption model and experimental results is confirmed and the simulation is validated.

5. Conclusion

This paper proposes a method for generating the speed trajectory that minimizes the vehicle's energy consumption between signals. By utilizing the floating car data, the proposed method can be applied even when vehicle communication is unavailable. A GMM was used to model the traffic flow relationship between adjacent signals using floating car data, and a method was proposed to determine the speed trajectory by combining the estimated values with DP. Simulation and experiment using a front-IWM-EV show that the method can reduce power consumption as an expected value. The proposed method can be straightforwardly extended to other EV prototypes.

An initial proposal for utilizing floating car data to derive the energy-optimized speed trajectory is presented. In the future, we will investigate the constraints imposed by the vehicles ahead, and the utilization of onboard vision information for the extension of the proposed method in practical applications.

Acknowledgment

This research was partly supported by Industrial Technology Research Grant Program from New Energy and Industrial Technology Development Organization (NEDO) of Japan (number 05A48701d), the Ministry of Education, Culture, Sports, Science and Technology grant (number 22246057 and 26249061), and Kashiwa ITS Promotion Council including Kanto Regional Development Bureau of the Ministry of Land, Infrastructure, Transport, and Tourism.

References

(1) Z. Wu, M. Wang, J. Zheng, X. Sun, M. Zhao, and X. Wang, "Life cycle greenhouse gas emission reduction potential of battery electric vehicle," *Journal of Cleaner Production*, vol. 190, pp. 462–470, 2018.

(2) Y. Zhang, X. Qu, and L. Tong, "Optimal eco-driving control of autonomous and electric trucks in adaptation to highway topography: Energy minimization and battery life extension," *IEEE Transactions on Transportation Electrification*, vol. 8, no. 2, pp. 2149–2163, 2022.

(3) M. Hattori, O. Shimizu, S. Nagai, H. Fujimoto, K. Sato, Y. Takeda, and T. Nagashio, "Quadrant dynamic programming for optimizing velocity of ecological adaptive cruise control," *IEEE/ASME Transactions on Mechatronics*, vol. 27, no. 3, pp. 1533–1544, 2022.

(4) H. Yang, F. Almutairi, and H. Rakha, "Eco-driving at signalized intersections: A multiple signal optimization approach," *IEEE Transactions on Intelligent Transportation Systems*, vol. 22, no. 5, pp. 2943–2955, 2021.

(5) Q. Lin, S. E. Li, S. Xu, X. Du, D. Yang, and K. Li, "Eco-driving operation of connected vehicle with v2i communication among multiple signalized intersections," *IEEE Intelligent Transportation Systems Magazine*, vol. 13, no. 1, pp. 107–119, 2021.

(6) Z. Bai, P. Hao, W. ShangGuan, B. Cai, and M. J. Barth, "Hybrid reinforcement learning-based eco-driving strategy for connected and automated vehicles at signalized intersections," *IEEE Transactions on Intelligent Transportation Systems*, vol. 23, no. 9, pp. 15850–15863, 2022.

(7) H. Yang, H. Rakha, and M. V. Ala, "Eco-cooperative adaptive cruise control at signalized intersections considering queue effects," *IEEE Transactions on Intelligent Transportation Systems*, vol. 18, no. 6, pp. 1575–1585, 2017.

(8) Z. Wang, G. Wu, and M. J. Barth, "Cooperative eco-driving at signalized intersections in a partially connected and automated vehicle environment," *IEEE Transactions on Intelligent Transportation Systems*, vol. 21, no. 5, pp. 2029–2038, 2020.

(9) A. S. M. Bakibillah, M. A. S. Kamal, C. P. Tan, T. Hayakawa, and J.-I. Imura, "Event-driven stochastic eco-driving strategy at signalized intersections from self-driving data," *IEEE Transactions on Vehicular Technology*, vol. 68, no. 9, pp. 8557–8569, 2019.

(10) ITS Division, National Institute for Land and Infrastructure Management, "ETC2.0:"ETC2.0" Probe information," `http://www.nilim.go.jp/lab/qcg/research/etc-2.0_en.html`, Accessed 27 Nov. 2022.

(11) R. Tang, R. Kanamori, and T. Yamamoto, "Short-term urban link travel time prediction using dynamic time warping with disaggregate probe data," *IEEE Access*, vol. 7, pp. 98959–98970, 2019.

(12) S. Axer and B. Friedrich, "Estimating signal phase and timing for traffic actuated intersections based on low frequency floating car data," in *2016 IEEE 19th International Conference on Intelligent Transportation Systems (ITSC)*, pp. 2059–2064, 2016.

(13) S. A. Fayazi, A. Vahidi, G. Mahler, and A. Winckler, "Traffic signal phase and timing estimation from low-frequency transit bus data," *IEEE Transactions on Intelligent Transportation Systems*, vol. 16, no. 1, pp. 19–28, 2015.

(14) H. Fujimoto and S. Harada, "Model-based range extension control system for electric vehicles with front and rear driving-braking force distributions," *IEEE Transactions on Industrial Electronics*, vol. 62, no. 5, pp. 3245–3254, 2015.